Archive of Applied Mechanics 74 (2004) 262 – 276 © Springer-Verlag 2004
DOI 10.1007/s00419-004-0348-3

Global structural behaviour of thin and moderately thick monoclinic spherical shells using a mixed shear deformation model

A. M. Zenkour

Summary The static and dynamic responses of anisotropic spherical shells under a uniformly distributed transverse load are investigated. Analytical solutions using the mixed variational formulation are presented for spherical shells subjected to various boundary conditions. Numerical results of a refined mixed first-order shear deformation theory for natural frequencies, critical buckling, center deflections and stresses are compared with those obtained using the classical shell theory. A variety of simply-supported and clamped boundary conditions are considered and comparisons with the existing literature are made. The sample numerical results presented herein for global structural behaviour of monoclinic spherical shells should serve as references for future comparisons.

Keywords Monoclinic spherical shells, mixed variational formulation, series solutions, refined shear deformation theory

1 Introduction

A wide application of anisotropic materials in modern technology enhanced a particular interest among researchers regarding the theory of anisotropic shells. Shells are widely used as structural elements in modern construction engineering, aircraft construction, shipbuilding, rocket construction, etc.

The static and dynamic analyses of shells have been studied for a long time. Shell structures can be subjected to external loads and displacements or to internal strains. These effects may cause large displacement responses with or without structural instabilities, both in the static and/or in the dynamic regime. Many shell theories have been developed over the last century, as well as methods to solve their governing equations [1–4]. Two-dimensional shell theories, such as the classical, first-order, and higher-order shear deformation theories, are mechanics-of-materials and applied elasticity approaches for the static and dynamic bending of plates and shells. These theories offer, in most situations if not all, accurate and reliable solutions for the analysis and design of shells and shell systems. The methods of solution are mostly exact closed-form solutions [5–7].

Here we will restrict our attention to the solution of anisotropic spherical shells. The open spherical shell has applications in a variety of aerospace and civil engineering structures. For example, Stephens and Fulton [8] have studied the axisymmetric response of shallow spherical caps due to step loading. Ball and Burt [9] have studied the asymmetric response of shallow spherical caps subjected to asymmetric step pressure loading. Reddy and Khdeir [10] have investigated the transient behaviour of cross-ply laminated composite spherical shells using a third-order shear deformation theory. However, the open spherical shell is perhaps the least widely studied of all existing shell models. This is primarily because very few researchers have attempted to include spherical shells in their models. In addition, most solutions existing in the literature are limited to cylindrical shells and/or sinusoidal distribution of the transverse load [7, 11–16].

Received 14 January 2003; accepted for publication 3 June 2004

A. M. Zenkour
Department of Mathematics, Faculty of Education,
Tanta University, Kafr El-Sheikh 33516, EGYPT
Fax: 002-047-3223415
e-mail: Zenkour@powernet.com.eg

The study of thin spherical shells usually involves the use of shell theories with emphasis on the development of solution methods. Spherical shells are often modeled using the classical shell theory neglecting transverse shear deformations. Refined shell theories allowing for a more adequate description of structural response characteristics are needed. They provide improved global response parameters for moderately thick shells when compared to the classical shell theory. Thick and moderately thick shells have a number of distinctly different features from thin shells. One of these features is that in thick shells the transverse shear deformation may no longer be neglected. In a number of particular cases of loadings the radial stress distribution of thick shells is very important and needs to be considered in the shell analysis.

It is not difficult to incorporate transverse shear deformations in shells. This can be accomplished following the work of Reissner [17] for plate theory. Nevertheless, it is not an easy task to incorporate radial stresses in thin shell theory and to obtain quadratic shear stress distributions through the shell thickness in order to describe the behaviour of thick shells. Attention in the previously developed shell theories was focused on two-dimensional shell equations while maintaining a linear stress distribution through the shell thickness (see Flügge [1]; Niordson [18]). It appears that refinement of the stress distribution in thick shells has hardly been ignored. The theory of thin shells may provide a good estimate of the strain energy for some problems in thick shells. Nevertheless, it cannot provide an accurate distribution for the stresses through the thickness. This accuracy is imperative from an engineering point of view.

The usual refined theory considered in the treatment of dynamic and static responses of anisotropic shells is the first-order transverse shear deformation theory [5, 13]. Comparison of the bending response of spherical shells obtained from the classical shell theory and first-order shear deformation shell theory would be interesting and useful as it would shed light on the relative importance of the inclusion of shear deformation effects. In the present analysis, the bending response of anisotropic spherical shells under a uniformly distributed transverse load is studied using a refined first-order shear deformation shell theory. The mixed variational formulation is used to obtain the governing equations and to develop the numerical solution for free vibration, buckling and bending of anisotropic spherical shells. The results obtained are compared with those obtained using classical shell theory. Comparisons with some of the available results (obtained for simply-supported edge conditions) are performed and appropriate conclusions concerning the various effects are formulated. The numerical results included here for monoclinic shells are not available in the literature and, therefore, should be of interest to designers of shell structures, numerical analysts and experimentalists in evaluating their techniques.

2
Mixed variational formulation

The variational method finds one of the most fruitful fields of application in the small displacement theory of elasticity. When the existence of a strain energy function is assured and the external forces are assumed to be kept unchanged during displacement variation, the principle of virtual work leads to the establishment of the principle of minimum potential energy. The variational principle is generalized by the introduction of Lagrange's multipliers to yield a family of variational principles that include the Hellinger–Reissner's principle, the principle of minimum complementary energy, and so forth [13–16, 19–22].

Variational formulations of elasticity find another important application as a computational tool. If the correct displacements are known to minimize some integral, then a finite linear combination of suitable functions can be inserted into the integral and the constants of combination can then be sought that provide the smallest possible value to the integral over the class of functions under consideration. The problem is thus reduced to an algebraic one that is well suited to modern computers. This approach is illustrated here based upon Hamilton's mixed variational formula in connection with the static and dynamic problems of anisotropic spherical shells.

The final form of the mixed variational formulation based upon Hamilton's principle is given by [13, 16, 19–22]:

$$0 = \int_{t_1}^{t_2} \left\{ \int\int\int_V \left[\rho \ddot{u}_i \delta u_i + \delta\left(\sigma_{ij}\varepsilon_{ij} - \bar{U}(\sigma)\right) \right] dv + \delta\Pi \right\} dt, \quad (i,j = 1,2,3), \tag{1}$$

where (t_1, t_2) is a time interval, ρ is the density of the undeformed body and $\bar{U}(\sigma)$ is the complementary energy density. The potential energy Π of the applied loads can be defined as a function of the displacement field u_i and the applied loads as follows:

$$\Pi = -\int\int\int_V B_i u_i dv - \int\int_{S_\sigma} F_i^* u_i ds - \int\int_{S_u} n_j \sigma_{ij}(u_i - u_i^*) ds, \quad (i,j = 1,2,3), \tag{2}$$

where n_j are the components of the unit vector along the outward normal to the total surface $S_\sigma + S_u$, B_i are the body forces measured per unit volume of the undeformed body, F_i^* are the prescribed components of the stress vector per unit area of the surface S_σ, and u_i^* are the prescribed components of the displacements of the remaining surface S_u. For stresses σ_{ij} and strains ε_{ij} $(i,j = 1,2,3)$ the subscripts 1–6 are defined as follows: $1 \to 11$, $2 \to 22$, $3 \to 33$, $4 \to 23$, $5 \to 13$, and $6 \to 12$. Then the first variation of the complementary energy density is given by:

$$\delta \bar{U}(\sigma) = a_{ij}\sigma_i \delta\sigma_j, \quad (i,j = 1,2,\ldots,6), \tag{3}$$

where $a_{ji} = a_{ij}$ are the coefficients of deformation (compliances). The utilization of the mixed variational principles allows one to treat the shell problems by introducing kinematic assumptions of any power of the thickness coordinate. Also, the transverse shear stresses are consistent with the surface conditions. So, the necessity for the introduction of a shear correction factor required in other first-order shear deformation theories is obviated. In addition, the effect of transverse normal stress is taken into account.

3
Derivation of the governing equations

The spherical shell as shown in Fig. 1 is assumed to be of length a, width b, radius of a value of the mid-surface R, and uniform thickness h. The orthogonal curvilinear coordinates (ξ_1, ξ_2, ζ) are taken such that the ξ_1- and ξ_2- curves are lines of curvature on the mid-surface $(\zeta = 0)$, and ζ- curves are straight lines perpendicular to the mid-surface and positive in a downward direction. Let the shell be subjected to a distributed transverse load q as well as to the compressive in-plane edge forces S_1 and S_2 and a distributed shear force S_6 (per unit length) acting on the mid-plane of the shell. Then, for the first variation of the potential energy Π in the absence of body forces and prescribed displacements we have

$$\delta\Pi = -\int\int_{S_\sigma} F_i^* \delta u_i ds = \int\int_{S_\sigma} \Big[-q + (S_1 \partial_{\bar{\xi}_1} w + S_6 \partial_{\bar{\xi}_2} w)\partial_{\bar{\xi}_1} + (S_6 \partial_{\bar{\xi}_1} w + S_2 \partial_{\bar{\xi}_2} w)\partial_{\bar{\xi}_2}\Big] \delta w d\bar{\xi}_1 d\bar{\xi}_2, \tag{4}$$

where $\partial_{\bar{\xi}_i} = \alpha_i \partial_{\xi_i}$, ∂_{ξ_i} denotes differentiation with respect to ξ_i and $\alpha_1 = \alpha_2 = \alpha$ is the surface metric of the spherical shell.

As in the shear deformation theory of flat plates, we start in the usual way by proposing the first-order displacement field:

$$\left.\begin{aligned} u_1(\xi_1,\xi_2,\zeta) &= (1+\zeta^*)\ u(\xi_1,\xi_2) + \zeta\psi(\xi_1,\xi_2), \\ u_2(\xi_1,\xi_2,\zeta) &= (1+\zeta^*)\ v(\xi_1,\xi_2) + \zeta\varphi(\xi_1,\xi_2), \\ u_3(\xi_1,\xi_2,\zeta) &= w(\xi_1,\xi_2), \end{aligned}\right\} \tag{5}$$

where $\zeta^* = \zeta/R$, (u, v, w) are the displacements of a point on the mid-surface, and ψ and φ are the rotations at $\zeta = 0$ of the normals to the mid-surface with respect to the ξ_2- and ξ_1- axes, respectively. The strain field for the assumed displacement field follows immediately as

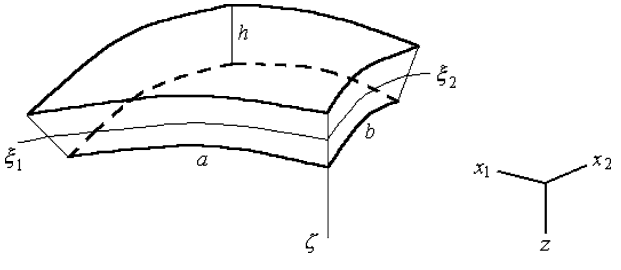

Fig. 1. Geometry and coordinates system of the spherical shell

$$\varepsilon_1 = w^* + \partial_{x_1} u + \zeta \partial_{x_1} \psi, \quad \varepsilon_4 = \varphi + \partial_{x_2} w,$$
$$\varepsilon_2 = w^* + \partial_{x_2} v + \zeta \partial_{x_2} \varphi, \quad \varepsilon_5 = \psi + \partial_{x_1} w, \tag{6}$$
$$\varepsilon_3 = 0, \quad \varepsilon_6 = \partial_{x_1} v + \partial_{x_2} u + \zeta(\partial_{x_1} \varphi + \partial_{x_2} \psi).$$

Here, $w^* = w/R$ and x_i denote the Cartesian coordinates, $dx_i = \alpha d\xi_i,\ i = 1, 2$ (see [5]). The non-vanishing stress field is assumed to be of the form [13, 19–21]:

$$\sigma_i = [G_i^{(0)}(\xi_1, \xi_2) + \zeta G_i^{(1)}(\xi_1, \xi_2)](1 + \zeta^*)^{-1},$$
$$\sigma_j = G_j^{(0)}(\xi_1, \xi_2)[1 - \bar{\zeta}^2](1 + \zeta^*)^{-1}, \tag{7}$$
$$\sigma_3 = \sum_{r=0}^{3} \zeta^r G_3^{(r)}(\xi_1, \xi_2), \quad (i = 1, 2, 6;\ j = 4, 5),$$

where $\bar{\zeta} = 2\zeta/h$. The functions $G_i^{(0)}, G_i^{(1)}$ and $G_j^{(0)}$ may be obtained easily from the condition that the above stress field satisfies the following stress resultants:

$$\{N_i, M_i, Q_j\} = \int_{-h/2}^{+h/2} \{\sigma_i, \zeta\sigma_i, \sigma_j\}(1 + \zeta^*) d\zeta, \quad (i = 1, 2, 6;\ j = 4, 5). \tag{8}$$

Also, the functions $G_3^{(r)}$ follow from the requirement that the transverse normal stress σ_3 satisfies the conditions

$$\sigma_{3_{|z=+h/2}} = 0, \quad \sigma_{3_{|z=-h/2}} = -q, \quad \int_{-h/2}^{+h/2} \sigma_3 d\zeta = 0, \quad \int_{-h/2}^{+h/2} \zeta\sigma_3 d\zeta = 0. \tag{9}$$

Therefore, the final expressions for the stress components can be written in terms of their resultants and the thickness coordinate ζ:

$$\sigma_i = N_i/h + 12M_i\zeta/h^3, \quad \sigma_j = 3Q_j(1 - \bar{\zeta}^2)/2h, \quad (j = 4, 5),$$
$$\sigma_3 = (q/4)[1 - 2\bar{\zeta} - 5\bar{\zeta}^2](1 - \bar{\zeta}), \quad (i = 1, 2, 6). \tag{10}$$

It is to be noted that the transverse shear stresses σ_4 and σ_5 are functions of ζ and vanish on the faces $\zeta = \pm h/2$.

3.1
Equations of equilibrium (motion)

The next step in deriving the governing equations consists of the substitution of Eqs. (5), (6), and (10) into the mixed variational formulation (Eq. 1). The extremum condition gives the following equilibrium (dynamic) equations:

$$\partial_{x_1} N_1 + \partial_{x_2} N_6 = 0\ (I_1\ddot{u} + I_2\ddot{\psi}), \quad \partial_{x_1} N_6 + \partial_{x_2} N_2 = 0\ (I_1\ddot{v} + I_2\ddot{\varphi}),$$
$$\partial_{x_1} \bar{Q}_5 + \partial_{x_2} \bar{Q}_4 - \bar{N}_1 - \bar{N}_2 + q = 0 \quad (I_0\ddot{w}), \tag{11}$$
$$\partial_{x_1} M_1 + \partial_{x_2} M_6 - Q_5 = 0(I_2\ddot{u} + I_3\ddot{\psi}), \quad \partial_{x_1} M_6 + \partial_{x_2} M_2 - Q_4 = 0\ (I_2\ddot{v} + I_3\ddot{\varphi}),$$

where

$$\bar{N}_i = N_i/R, \quad \bar{Q}_4 = Q_4 + (S_6\partial_{x_1} + S_2\partial_{x_2})w, \quad \bar{Q}_5 = Q_5 + (S_1\partial_{x_1} + S_6\partial_{x_2})w, \tag{12}$$

and inertia $I_j\ (j = 0, 1, 2, 3)$ is given by

$$\{I_0, I_1, I_2, I_3\} = \int_{-h/2}^{+h/2} \rho\{1, (1 + \zeta^*)^2, \zeta(1 + \zeta^*), \zeta^2\} d\zeta. \tag{13}$$

Eq. (11) can be specialized to flat plates by setting $1/R = 0$. The classical shell theory can be obtained by setting $\varphi = -\partial_{x_2} w$ and $\psi = -\partial_{x_1} w$.

3.2
Boundary conditions

Requirments of the Kinematic and dynamic boundary conditions are given below:

At edge $x_1 = 0, a$	*At edge* $x_2 = 0, b$
u = prescribed; otherwise $N_1 = 0$	u = prescribed; otherwise $N_6 = 0$
v = prescribed; otherwise $N_6 = 0$	v = prescribed; otherwise $N_2 = 0$
w = prescribed; otherwise $\bar{Q}_5 = 0$	w = prescribed; otherwise $\bar{Q}_4 = 0$
ψ = prescribed; otherwise $M_1 = 0$	ψ = prescribed; otherwise $M_6 = 0$
φ = prescribed; otherwise $M_6 = 0$	φ = prescribed; otherwise $M_2 = 0$

3.3
Constitutive equations

The constitutive equations are given by:

$$\begin{Bmatrix} N_1 \\ N_2 \\ N_6 \end{Bmatrix} = \begin{bmatrix} A_{11} & A_{12} & A_{16} \\ A_{12} & A_{22} & A_{26} \\ A_{16} & A_{26} & A_{66} \end{bmatrix} \begin{Bmatrix} w^* + \partial_{x_1} u \\ w^* + \partial_{x_2} v \\ \partial_{x_1} v + \partial_{x_2} u \end{Bmatrix}, \tag{14}$$

$$\begin{Bmatrix} Q_4 \\ Q_5 \end{Bmatrix} = \begin{bmatrix} A_{44} & A_{45} \\ A_{45} & A_{55} \end{bmatrix} \begin{Bmatrix} \varphi + \partial_{x_2} w \\ \psi + \partial_{x_1} w \end{Bmatrix}, \tag{15}$$

$$\begin{Bmatrix} M_1 \\ M_2 \\ M_6 \end{Bmatrix} = \begin{bmatrix} D_{11} & D_{12} & D_{16} \\ D_{12} & D_{22} & D_{26} \\ D_{16} & D_{26} & D_{66} \end{bmatrix} \begin{Bmatrix} \partial_{x_1} \psi \\ \partial_{x_2} \varphi \\ \partial_{x_1} \varphi + \partial_{x_2} \psi \end{Bmatrix}, \tag{16}$$

where

$$\begin{bmatrix} A_{11} & A_{12} & 0 & 0 & A_{16} \\ & A_{22} & 0 & 0 & A_{26} \\ & & A_{44} & A_{45} & 0 \\ & & & A_{55} & 0 \\ \text{symm.} & & & & A_{66} \end{bmatrix} = h \begin{bmatrix} a_{11} & a_{12} & 0 & 0 & a_{16} \\ & a_{22} & 0 & 0 & a_{26} \\ & & \frac{6}{5}a_{44} & \frac{6}{5}a_{45} & 0 \\ & & & \frac{6}{5}a_{55} & 0 \\ \text{symm.} & & & & a_{66} \end{bmatrix}^{-1}, \quad D_{ij} = \frac{h^2}{12} A_{ij}.$$

For monoclinic shell, when we have one plane of elastic symmetry parallel to the median surface of the shell, the compliances a_{ij} may be expressed in terms of the engineering characteristics as [23]:

$$\begin{aligned} &a_{11} = \frac{1}{E_1}, \quad a_{12} = -\frac{\nu_{12}}{E_1} = -\frac{\nu_{21}}{E_2}, \quad a_{16} = \frac{\eta_{16}}{E_1} = \frac{\eta_{61}}{G_{12}}, \quad a_{26} = \frac{\eta_{26}}{E_2} = \frac{\eta_{62}}{G_{12}}, \\ &a_{22} = \frac{1}{E_2}, \quad a_{44} = \frac{1}{G_{23}}, \quad a_{45} = \frac{\mu_{45}}{G_{23}} = \frac{\mu_{54}}{G_{13}}, \quad a_{55} = \frac{1}{G_{13}}, \quad a_{66} = \frac{1}{G_{12}}. \end{aligned} \tag{17}$$

Here, E_i, G_{ij} and ν_{ij} stand for Young's moduli, shear moduli and Poisson's ratios, respectively. Traditionally, the following notations are used: η_{61} and η_{62} are constants characterizing normal deformations in directions x_1 and x_2 when a shear load is applied in the $x_1 - x_2$ plane, and μ_{45} is the constant characterizing shear deformation in the plane $x_1 - \zeta$ when a shear load is applied in the plane $x_2 - \zeta$. This system of notations extends logically the notations for Poisson's ratios of an orthotropic material. In addition, for an orthotropic shell ($a_{16} = a_{26} = a_{45} = 0$) we find:

$$\begin{aligned} &A_{11} = \frac{hE_1}{1 - \nu_{12}\nu_{21}}, \quad A_{12} = \frac{hE_2\nu_{12}}{1 - \nu_{12}\nu_{21}} = \frac{hE_1\nu_{21}}{1 - \nu_{12}\nu_{21}}, \quad A_{22} = \frac{hE_2}{1 - \nu_{12}\nu_{21}}, \\ &A_{44} = \frac{5}{6} hG_{23}, \quad A_{55} = \frac{5}{6} hG_{13}, \quad A_{66} = hG_{12}. \end{aligned} \tag{18}$$

4
Solution procedure

The mixed variational formulation will be extended here in order to analyze the free vibration, the buckling and the bending problems of anisotropic spherical shells. For the free vibration case we set q, S_1, S_2, and S_6 in the governing equations equal to zero, and represent the displacement quantities as:

$$\begin{Bmatrix} (u,\psi) \\ w \\ (v,\varphi) \end{Bmatrix} = \sum_{i=1}^{n}\sum_{j=1}^{n} \begin{Bmatrix} (U_{ij},\Psi_{ij})\ F'(\lambda_i x_1)\ G(\lambda_j x_2) \\ W_{ij}\ F(\lambda_i x_1)\ G(\lambda_j x_2) \\ (V_{ij},\Phi_{ij})\ F(\lambda_i x_1)\ G'(\lambda_j x_2) \end{Bmatrix} e^{\hat{i}\omega t}, \tag{19}$$

where $\omega = \omega_{ij}$ denotes the eigenfrequency associated with the (ith, jth) eigenmode, $\hat{i} = \sqrt{-1}$, and $U_{ij}, V_{ij}, W_{ij}, \Phi_{ij}$ and Ψ_{ij} are arbitrary parameters. The functions $F(\lambda_i x_1)$ and $G(\lambda_j x_2)$ can be constructed for any combination of simply-supported and/or clamped boundary conditions on the shell edges (see [14, 15]). Substitution of the constitutive equations (Eqs. 14–16), considered in conjunction with Eq. (19) in the final form of the mixed variational formulation given in Eq. (1), yields a system of algebraic equations. For the free vibration case ($q = S_1 = S_2 = S_6 = 0$) this system is expressed in compact form as:

$$[K]\{\Delta\} = \omega^2[L]\{\Delta\}, \tag{20}$$

and for buckling ($\omega \to 0,\ q = S_6 = 0,\ S_1 = -\beta_\gamma,\ S_2 = -\gamma\beta_\gamma,\ \gamma = S_2/S_1$), we obtain

$$[K]\{\Delta\} = \beta_\gamma[N]\{\Delta\}, \tag{21}$$

where $\{\Delta\}$ denotes the column

$$\{\Delta\}^{\mathrm{T}} = \{U_{ij}, V_{ij}, W_{ij}, \Phi_{ij}, \Psi_{ij}\}. \tag{22}$$

The elements of the coefficient matrices $[K]$, $[L]$ and $[N]$ are defined in the Appendix.

For non-trivial solutions of Eqs. (20) and (21), the following determinants should be zero:

$$\left|[K] - \omega^2[L]\right| = 0 \text{ and } \left|[K] - \beta_\gamma[N]\right| = 0. \tag{23}$$

The above equations give the eigenfrequencies and the critical buckling loads.

For bending analysis, a uniformly distributed transverse load with a total of n terms in both x_1 and x_2 directions is used:

$$q(x_1,x_2) = \sum_{i=1}^{n}\sum_{j=1}^{n} q_{ij}\ \sin\frac{i\pi x_1}{a}\ \sin\frac{j\pi x_2}{b}, \tag{24}$$

where the coefficients q_{ij} are defined as follows:

$$q_{ij} = \frac{16q_0}{ij\pi^2}\begin{cases} 1 & i,j = 1,3,5,\ldots,n \\ 0 & \text{otherwise} \end{cases} \tag{25}$$

in which q_0 is the intensity of the load. In this case, Eq. (20) takes the form

$$[K]\{\Delta\} = \{F\}, \tag{26}$$

where $\{F\}$ denotes the load vector

$$\{F\}^{\mathrm{T}} = \{0, 0, q_{ij}f_0g_0, 0, 0\}, \tag{27}$$

and

$$f_0 = \int_0^a F(\lambda_i x_1)\ \sin\frac{i\pi x_1}{a}\ dx_1, \quad g_0 = \int_0^b G(\lambda_j x_2)\ \sin\frac{j\pi x_2}{b}\ dx_2. \tag{28}$$

Table 1. Center deflection ($wE/100q_0$) of an isotropic spherical shell under point load at the center, $a/h = 320$ (finite-element solution of Yang [25]: 38.670)

Theory	$n^a = 9$	$n = 49$	$n = 99$	$n = 149$	$n = 199$	$n = 249$
Vlasov [24]			39.560			
FSDT[b]	32.594	39.469	39.724	39.786	39.814	39.832
CST[b]			39.591		39.647	39.653
HSDT[c]	32.584	39.458	39.714	39.775	39.803	
MFST	32.5837	39.4580	39.7136	39.7747	39.8033	39.8210
CST	32.5630	39.3594	39.5806	39.6216	39.6360	39.6426

[a] $n \times n$ term series,
[b] Reddy [5],
[c] Reddy and Liu [6].

Thus, one needs to solve the 5×5 matrix equation, Eq. (26), for the vector of amplitudes of the generalized displacements.

5
Discussion of the results

In order to simplify the presentation, the edge conditions for spherical shells are denoted by the letters S (simply-supported) and C (clamped). For example, the designation CSCC denotes that the shell is clamped at $x_1 = 0$, simply-supported at $x_1 = a$, clamped at $x_2 = 0$ and $x_2 = b$. In addition, we will assume in all cases (unless otherwise stated) that $a/b = 1$ and $R/a = 5$.

5.1
Isotropic spherical shells

The bending of an isotropic SSSS spherical shell under point load at the center is analyzed. The following geometric and material parameters are used:

$$R/a = 3, \quad b/a = 1, \quad \nu = 0.3.$$

A comparison of the center deflection of the present theories (MFST and CST) with that obtained by Vlasov [24] is presented in Table 1. The results obtained using the first-order shear deformation theory (FSDT) of Reddy [5] and higher-order shear deformation theory (HSDT) of Reddy and Liu [6] are also presented. This problem was also solved using the finite element method by Yang [25]. The numerical solutions of Vlasov [24] and Yang [25] are taken from Reddy's paper [5] and both of them did not consider transverse shear strains. It is clear from the results that the series solution converges very slowly. The difference between the values

Table 2. Center deflection ($wE/100q_0$) of an isotropic spherical shell under point load at the center

a/h	*Theory*	$n = 9$	$n = 49$	$n = 99$	$n = 149$	$n = 199$	$n = 249$
100	FSDT[a]	3.6640	3.9019	3.9194	3.9270	3.9319	3.9356
	HSDT[b]	3.6610	3.8986	3.9158	3.9230	3.9274	
	MFST	3.6607	3.8986	3.9161	3.9237	3.9286	3.9323
	CST	3.6458	3.8588	3.8656	3.8668	3.8673	3.8675
20	FSDT[a]	0.1646	0.1713	0.1735	0.1748	0.1757	0.1764
	HSDT[b]	0.1637	0.1701	0.1715	0.1720	0.1722	
	MFST	0.1637	0.1704	0.1726	0.1739	0.1748	0.1755
	CST	0.1583	0.1600	0.1601	←		
10	FSDT[a]	0.03485	0.03755	0.03864	0.03927	0.03972	0.0400
	HSDT[b]	0.03450	0.03668	0.03704	0.03713	0.03716	
	MFST	0.0345	0.0372	0.0383	0.0389	0.0394	0.0397
	CST	0.0310	0.0312	←			
5	FSDT[a]	0.00671	0.00798	0.008523	0.008838	0.009061	0.0092
	HSDT[b]	0.00658	0.00775	0.007337	0.007350	0.007354	
	MFST	0.0066	0.0079	0.0085	0.0088	0.0090	0.0092
	CST	0.0046	←				

[a] Reddy [5],
[b] Reddy and Liu [6].

Table 3. Center deflection $(wE/100q_0)$ of an isotropic spherical shell under uniformly distributed load

n	*Theory*	a/h				
		320	100	20	10	5
9	FSDT[a]	—	314.28	49.701	11.266	1.9774
	HSDT[b]	—	314.33	49.526	10.873	1.6669
	MFST	928.99	314.25	49.370	11.138	1.9495
	CST	928.96	314.30	49.194	10.748	1.6434
49	FSDT[a]	—	313.87	49.695	11.265	1.9767
	HSDT[b]	—	313.93	49.523	10.872	1.6669
	MFST	916.96	313.84	49.364	11.137	1.9488
	CST	916.95	313.90	49.191	10.748	1.6433
99	FSDT[a]	—	313.86	49.695	11.265	1.9767
	HSDT[b]	—	313.93	49.523	10.872	1.6669
	MFST	916.96	313.84	49.364	11.137	1.9488
	CST	916.95	313.90	49.191	10.748	1.6433

[a] Reddy [5],
[b] Reddy and Liu [6].

predicted by MFST and CST is not significant because the shell is essentially very thin and shallow ($a/h = 320$ and $R/h = 960$). In addition, it can be seen that there is excellent agreement between the results obtained by MFST and those obtained by HSDT of Reddy and Liu [6].

To investigate the effect of transverse shear strains on the center deflection, the same spherical shell problem with point load at the center or uniformly distributed loading is analyzed, and the results are presented in Tables 2 and 3. Note that for the point load, the results obtained using MFST compare well with those obtained using HSDT and FSDT. The difference between the values predicted by MFST and CST increases with the decrease of the a/h ratio. For a uniformly distributed load, the solution given by the 49-term series is the same as that given by the 199-term series, indicating that the convergence is achieved with 49 (or less) terms in the series. Comparison of the MFST results with the CST results shows that the shear deformation is significant for side-to-thickness ratios smaller than 10. For example, the relative error between the two theories reaches 18.59% for $a/h = 5$.

5.2
Orthotropic spherical shells

Of great practical importance is a shell made of orthotropic material, i.e., a material through each point of which pass three mutually perpendicular planes of elastic symmetry. In this example numerical results will be presented for orthotropic spherical shell under uniformly distributed loading with a 45-term series. To complete the analysis, the results of free vibration and buckling problems are also presented. The numerical results obtained using MFST and CST will be compared, as a special case, with the exact closed form solution presented by Srinivas and Rao [26] for flat plate. The material properties used in this example are:

$$E_1 = 145.81\text{GPa}, \quad E_2 = 76.58\text{GPa}, \quad E_3 = 70\text{GPa}, \quad G_{12} = 35.7\text{GPa},$$
$$G_{13} = 25.97\text{GPa}, \quad G_{23} = 43.33\text{GPa}, \quad \nu_{12} = \nu_{13} = 0.44, \quad \nu_{32} = 0.23.$$

The following normalization is used:

$$\hat{\Omega} = \omega h \sqrt{\frac{\rho h}{A_{11}}}, \quad \hat{\beta}_\gamma = \frac{\beta_\gamma a^2}{h^3 E_1}, \quad \hat{w} = w\left(\frac{a}{2}, \frac{b}{2}\right) \frac{A_{11}}{q_0 h^2},$$
$$\hat{\sigma}_1 = \sigma_1\left(\frac{a}{2}, \frac{b}{2}, \frac{h}{2}\right) \frac{1}{q_0}, \quad \hat{\sigma}_2 = \sigma_2\left(\frac{a}{2}, \frac{b}{2}, \frac{h}{2}\right) \frac{1}{q_0}, \quad \hat{\sigma}_5 = \sigma_5\left(0, \frac{b}{2}, 0\right) \frac{1}{q_0}.$$

Tables 4 and 5 display the eigenfrequencies and critical buckling loads obtained using the present theories and deleting the stretching effects. The exact three-dimensional elasticity solutions of Srinivas and Rao [26] for SSSS square plates are used to assess improvement of frequency prediction. The results obtained from the higher-order shear deformation theory (HSDT) developed by Reddy [27], and from the theory referred to as DT developed by Librescu

Table 4. Eigenfrequencies $\hat{\Omega}$ of SSSS orthotropic spherical shells $(a/h = 10)$

R/a	*Theory*	(i,j)								
		(1,1)	(1,2)	(2,2)	(1,3)	(2,3)	(1,4)	(3,3)	(4,1)	(2,4)
5	MFST	0.0551	0.1069	0.1714	0.1903	0.2481	0.2962	0.3309	0.3311	0.3457
	CST	0.0567	0.1132	0.1944	0.2088	0.2892	0.3383	0.4181	0.4479	0.4161
10	MFST	0.0494	0.1041	0.1697	0.1888	0.2469	0.2953	0.3301	0.3303	0.3449
	CST	0.0512	0.1107	0.1929	0.2075	0.2883	0.3375	0.4174	0.4473	0.4155
20	MFST	0.0479	0.1034	0.1693	0.1884	0.2467	0.2951	0.3298	0.3301	0.3447
	CST	0.0498	0.1100	0.1926	0.2072	0.2880	0.3373	0.4173	0.4472	0.4153
50	MFST	0.0475	0.1032	0.1692	0.1883	0.2466	0.2950	0.3298	0.3300	0.3447
	CST	0.0493	0.1098	0.1925	0.2071	0.2880	0.3372	0.4172	0.4472	0.4153
100	MFST	0.0474	0.1032	0.1691	0.1883	0.2466	0.2950	0.3298	0.3300	0.3447
	CST	0.0493	0.1098	0.1925	0.2071	0.2879	0.3372	0.4172	0.4472	0.4153
Plate	MFST	0.0474	0.1032	0.1691	0.1883	0.2465	0.2949	0.3299	0.3300	0.3446
	CST	0.0493	0.1098	0.1925	0.2071	0.2879	0.3372	0.4172	0.4472	0.4153
	Exact[a]	0.0474	0.1033	0.1694	0.1888	0.2475	0.2969	0.3320	0.3319	0.3476
	HSDT[b]	0.0474	0.1033	0.1695	0.1888	0.2477	0.2969	0.3326	0.3330	0.3479
	DT[c]	0.0474	0.1033	0.1692	0.1884	0.2469	0.2958	0.3310	0.3310	0.3462

[a] Srinivas and Rao [26],
[b] Reddy [27],
[c] Librescu *et al.* [28].

Table 5. Non-dimensional critical buckling loads $\hat{\beta}_\gamma$ of SSSS orthotropic spherical shells

R/a	*Theory*	*a/h*=2		*a/h*=5		*a/h*=10		*a/h*=20		*a/h*=50	
		γ=0	γ=1	γ=0	γ=1	γ=0	γ=1	γ=0	γ=1	γ=0	γ=1
5	MFST	0.9795	0.4897	2.3225	1.1613	3.4678	1.7339	6.3132	3.1566	25.189	12.594
	CST	2.8189	1.4094	3.0072	1.5036	3.6796	1.8398	6.3695	3.1847	25.198	12.599
10	MFST	0.9526	0.4763	2.1544	1.0772	2.7954	1.3977	3.6233	1.8117	8.3777	4.1889
	CST	2.7920	1.3960	2.8390	1.4195	3.0072	1.5036	3.6796	1.8398	8.3869	4.1935
20	MFST	0.9459	0.4729	2.1124	1.0562	2.6272	1.3136	2.9509	1.4754	4.1748	2.0874
	CST	2.7852	1.3926	2.7970	1.3985	2.8390	1.4195	3.0072	1.5036	4.1840	2.0920
50	MFST	0.9440	0.4720	2.1006	1.0503	2.5802	1.2901	2.7626	1.3813	2.9980	1.4990
	CST	2.7834	1.3917	2.7852	1.3926	2.7920	1.3960	2.8189	1.4094	3.0072	1.5036
100	MFST	0.9437	0.4719	2.0989	1.0495	2.5734	1.2867	2.7357	1.3678	2.8299	1.4149
	CST	2.7831	1.3915	2.7836	1.3918	2.7852	1.3926	2.7920	1.3960	2.8390	1.4195
Plate	MFST	0.9436	0.4718	2.0984	1.0492	2.5712	1.2856	2.7267	1.3633	2.7738	1.3869
	CST	2.7830	1.3915	2.7830	1.3915	2.7830	1.3915	2.7830	1.3915	2.7830	1.3915
	HSDT[a]	0.9581	0.4791	2.0999	1.0500	2.5706	1.2853	2.7258	1.3629	2.7729	1.3864
	DT [b]	0.9435	0.4718	2.0978	1.0489	2.5704	1.2852	2.7258	1.3629	2.7729	1.3864

[a] Reddy [27],
[b] Librescu *et al.* [28].

et al. [28], are also used in the comparisons. Note that the results obtained using MFST are found to be in excellent agreement with relative errors between MFST and CST increasing slightly with the increase of the radius-to-side ratio. In addition, this relative error increases rapidly with the increase of the eigenmode values (see Table 4) and decreases rapidly with the increase of the side-to-thickness ratio (see Table 5).

Table 6 contains the non-dimensionalized center deflections $\hat{w}$ of orthotropic spherical shells under uniformly distributed load. The results are tabulated for various thickness-to-side, radius-to-side and aspect ratios. The deviation between MFST and CST increases with the increase of h/a, a/b and R/a ratios. This deviation is 0.76% at $h/a = 0.05$, $a/b = 0.5$ and $R/a = 5$ while at $h/a = 0.14$, $a/b = 2.0$ and $R/a = 100$, a deviation of 24.3% is observed. This is to be expected as the inclusion of transverse shear would have more effect on a thicker shell than on a thinner shell. In Table 7 the stresses $\hat{\sigma}_1$, $\hat{\sigma}_2$ and $\hat{\sigma}_5$ are presented for square shells with various values of thickness-to-side and radius-to-side ratios. The results in Tables 6 and 7, calculated in the present MFST and in Srinivas and Rao [26], are compared for flat plates. There

Table 6. Non-dimensionalized center deflection ($\hat{w}$) of SSSS orthotropic spherical shells under uniformly distributed load ($s = a/b$)

R/a	*Theory*	$h/a = 0.05$			$h/a = 0.10$			$h/a = 0.14$		
		$s = 0.5$	$s = 1.0$	$s = 2.0$	s = 0.5	$s = 1.0$	$s = 2.0$	s = 0.5	$s = 1.0$	$s = 2.0$
5	MFST	11816	7186.8	1846.7	1161.5	615.65	135.63	347.54	179.77	39.517
	CST	11727	7101.2	1797.3	1105.5	577.02	121.05	313.31	157.88	31.914
10	MFST	17914	9388.3	1995.7	1337.9	669.37	138.72	376.70	188.49	40.036
	CST	17688	9232.4	1936.8	1262.9	623.38	123.44	336.51	164.42	32.236
20	MFST	20507	10158.8	2036.6	1390.3	684.25	139.52	384.74	190.80	40.168
	CST	20206	9974.0	1975.1	1309.2	636.12	124.05	342.84	166.14	32.318
50	MFST	21367	10397.1	2048.3	1405.7	688.54	139.74	387.06	191.46	40.205
	CST	21039	10203.0	1986.0	1322.8	639.78	124.22	344.84	166.63	32.341
100	MFST	21496	10432.0	2050.0	1408.0	689.15	139.77	387.39	191.55	40.210
	CST	21164	10236.5	1987.6	1324.7	640.31	124.25	344.92	166.70	32.344
Plate	MFST	21539	10443.7	2050.6	1408.7	689.36	139.78	387.50	191.58	40.212
	CST	21206	10247.7	1988.1	1325.4	640.48	124.26	345.00	166.72	32.345
	Exact [a]	21542	10443.0	2048.7	1408.5	688.75	139.08	387.23	191.07	39.790

[a] Srinivas and Rao [26].

Table 7. Non-dimensionalized stresses of SSSS orthotropic spherical shells under uniformly distributed load

		h/a=0.05			h/a=0.10			h/a=0.14		
R/a	*Theory*	$\hat{\sigma}_1$	$\hat{\sigma}_2$	$\hat{\sigma}_5$	$\hat{\sigma}_1$	$\hat{\sigma}_2$	$\hat{\sigma}_5$	$\hat{\sigma}_1$	$\hat{\sigma}_2$	$\hat{\sigma}_5$
5	MFST	119.13	81.253	8.3393	35.565	23.505	5.0492	18.413	12.282	3.7324
	CST	119.82	81.148	—	36.007	23.120	—	18.804	11.862	—
10	MFST	143.58	92.869	10.1748	36.697	23.495	5.3854	18.499	12.045	3.8712
	CST	144.03	92.478	—	37.087	23.065	—	18.891	11.631	—
20	MFST	147.95	92.695	10.8169	36.451	22.922	5.4786	18.303	11.760	3.9080
	CST	148.35	92.261	—	36.864	22.520	—	18.724	11.377	—
50	MFST	146.59	89.867	11.0154	36.020	22.390	5.5054	18.108	11.535	3.9184
	CST	147.01	89.472	—	36.466	22.022	—	18.555	11.180	—
100	MFST	145.41	88.460	11.0446	35.830	22.182	5.5092	18.030	11.452	3.9199
	CST	145.86	88.089	—	36.290	21.829	—	18.487	11.108	—
Plate	MFST	143.89	86.828	11.0543	35.617	21.959	5.5105	17.945	11.365	3.9204
	CST	144.37	86.488	—	36.092	21.622	—	18.414	11.032	—
	Exact [a]	144.31	87.080	10.8730	36.021	22.210	5.3411	18.346	11.615	3.7313

[a] Srinivas and Rao [26].

is excellent agreement in the deflection $\hat{w}$ and the in-plane stress $\hat{\sigma}_2$. However, a minor deviation may be observed for the stresses $\hat{\sigma}_1$ and $\hat{\sigma}_5$.

5.3 Monoclinic spherical shells

This example utilizes the following monoclinic material [23]:

$$E_1 = 47.9\text{GPa}, \quad E_2 = 8.6\text{GPa}, \quad G_{23} = 3.81\text{GPa}, \quad G_{13} = 19.6\text{GPa}, \quad G_{12} = 0.837\text{GPa},$$
$$E_3 = 30.4\text{GPa}, \quad \nu_{12} = 0.361, \quad \mu_{16} = 1.25, \quad \mu_{26} = 0.036, \quad \mu_{45} = -0.071,$$
$$\nu_{13} = 0.509, \quad \nu_{23} = 0.052, \quad \eta_{36} = 0.044.$$

The following normalization is used in the presentation of the numerical results in Table 8 and Figs. 2–8:

$$\bar{\Omega} = \omega \frac{a^2}{h}\sqrt{\frac{\rho}{E_2}}, \quad \bar{\beta}_\gamma = \frac{\beta_\gamma a^2}{h^3 E_2}, \quad \bar{w} = w\left(\frac{a}{2},\frac{b}{2}\right)\frac{10^2 h^3 E_2}{q_0 a^4}, \quad \bar{\sigma}_1 = \sigma_1\left(\frac{a}{2},\frac{b}{2},\frac{h}{2}\right)\frac{h^2}{q_0 a^2},$$
$$\bar{\sigma}_2 = \sigma_2\left(\frac{a}{2},\frac{b}{2},\frac{h}{2}\right)\frac{h}{q_0 a}, \quad \bar{\sigma}_4 = \sigma_4\left(\frac{a}{2},0,0\right)\frac{h}{q_0 a}, \quad \bar{\sigma}_5 = \sigma_5\left(0,\frac{b}{2},0\right)\frac{h}{q_0 a}, \quad \bar{\sigma}_6 = \sigma_6\left(0,0,-\frac{h}{2}\right)\frac{h}{q_0 a}.$$

Table 8. Global structural behaviour of monoclinic square spherical shells (a/h=10)

BC	*Theory*	$\bar{\Omega}$	$\bar{\beta}_0$	$\bar{\beta}_1$	$\hat{w}$	$\bar{\sigma}_1$	$\bar{\sigma}_2$	$\bar{\sigma}_6$	$\bar{\sigma}_4$	$\bar{\sigma}_5$
SSSS	MFST	7.9756	6.6429	3.3215	2.3884	0.6986	1.4833	0.3753	0.2835	0.7101
	CST	8.0864	6.8287	3.4143	2.3336	0.7002	1.4854	0.3675	—	—
SSCS	MFST	8.7729	7.9963	3.6889	1.9882	0.5843	1.6011	—	—	0.6269
	CST	8.9287	8.2878	3.8234	1.9271	0.5822	1.6169	—	—	—
SSCC	MFST	9.8747	10.1119	4.5012	1.7428	0.5183	1.7894	—	—	0.5949
	CST	10.1633	10.7278	4.7754	1.6509	0.5066	1.8246	—	—	—
CSSS	MFST	11.5363	12.1208	6.5292	1.0864	0.4284	0.6237	—	0.2060	—
	CST	11.7995	12.7030	6.8428	1.0437	0.4299	0.6127	—	—	—
CSCS	MFST	12.2648	13.4545	6.7273	0.9887	0.3951	0.7827	—	—	—
	CST	12.5646	14.1418	7.0709	0.9474	0.3961	0.7809	—	—	—
CSCC	MFST	13.1204	15.2956	7.3980	0.9686	0.3912	1.0008	—	—	—
	CST	13.5162	16.2684	7.8686	0.9175	0.3889	1.0200	—	—	—
CCSS	MFST	15.3494	20.9611	11.6305	0.6292	0.3233	0.3380	—	0.1861	—
	CST	15.9811	22.9347	12.7256	0.5791	0.3228	0.3163	—	—	—
CCCS	MFST	16.1508	22.1822	11.4533	0.6067	0.3152	0.4739	—	—	—
	CST	16.8505	24.2572	12.5246	0.5594	0.3156	0.4541	—	—	—
CCCC	MFST	16.9141	23.9282	11.9641	0.6295	0.3314	0.6587	—	—	—
	CST	17.6915	26.2754	13.1377	0.5784	0.3314	0.6509	—	—	—

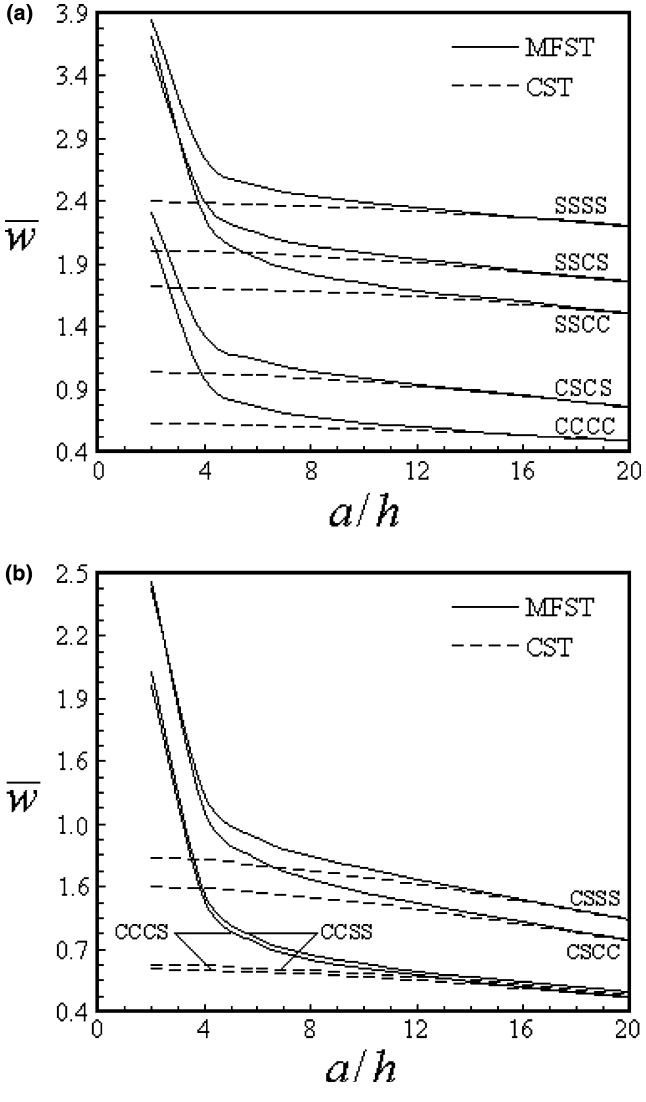

Fig. 2. Non-dimensional center deflection ($\bar{w}$) versus side-to-thickness ratio of monoclinic spherical shells for (a) SSSS, SSCS, SSCC, CSCS and CCCC boundary conditions, and (b) CSSS, CSCC, CCSS and CCCS boundary conditions

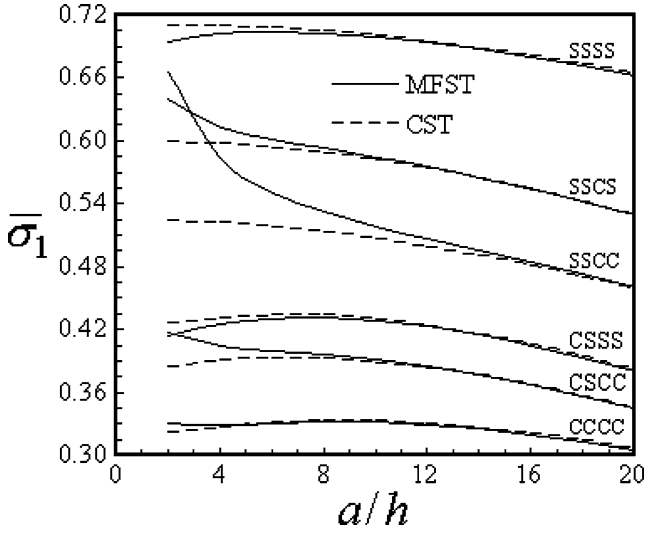

Fig. 3. Non-dimensional in-plane stress ($\bar{\sigma}_1$) versus side-to-thickness ratio of monoclinic spherical shells for various boundary conditions

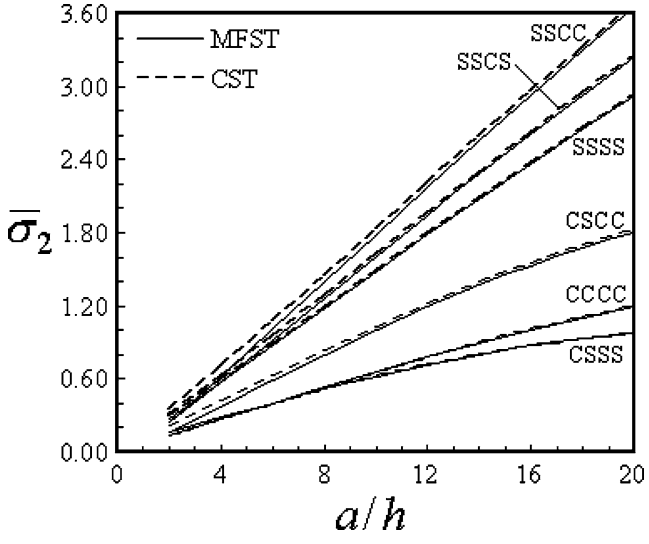

Fig. 4. Non-dimensional in-plane stress ($\bar{\sigma}_2$) versus side-to-thickness ratio of monoclinic spherical shells for various boundary conditions

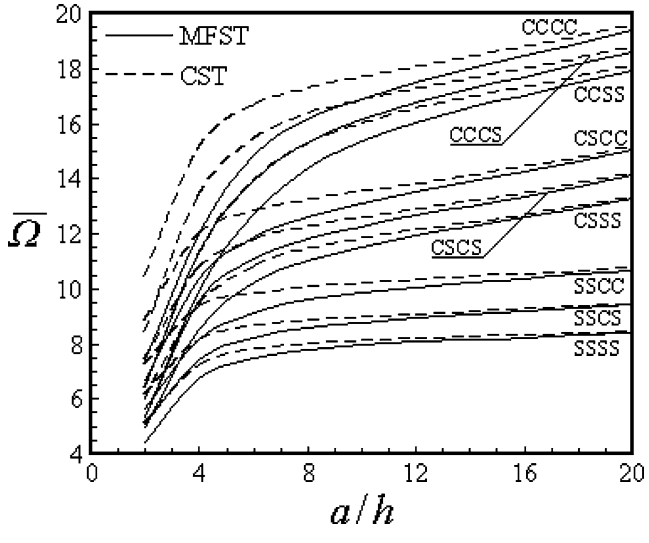

Fig. 5. Effect of *a/h* on the fundamental frequency $\bar{\Omega}$ of monoclinic spherical shells for various boundary conditions

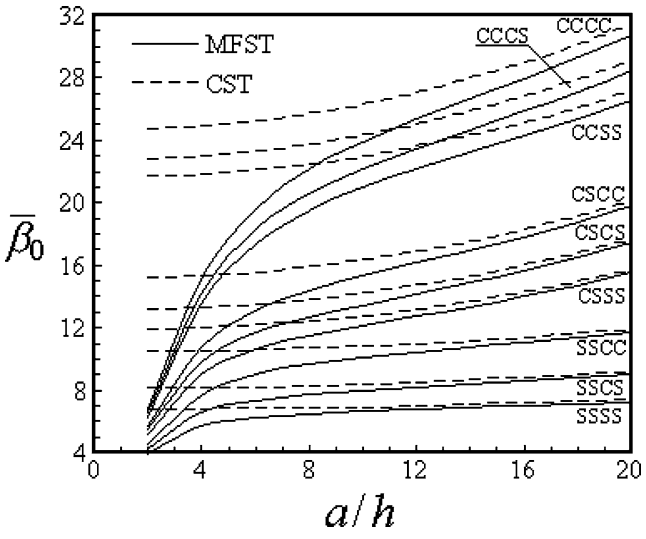

Fig. 6. Effect of *a/h* on the uniaxial critical buckling load $\bar{\beta}_0$ of monoclinic spherical shells for various boundary conditions

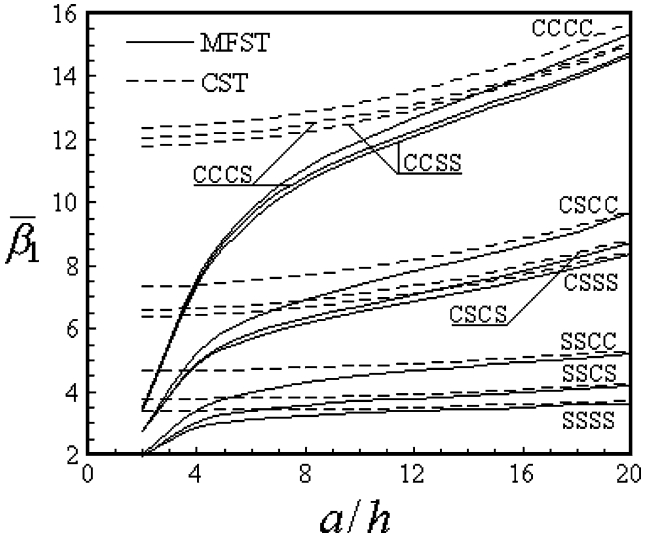

Fig. 7. Effect of *a/h* on the biaxial critical buckling load $\bar{\beta}_1$ of monoclinic spherical shells for various boundary conditions

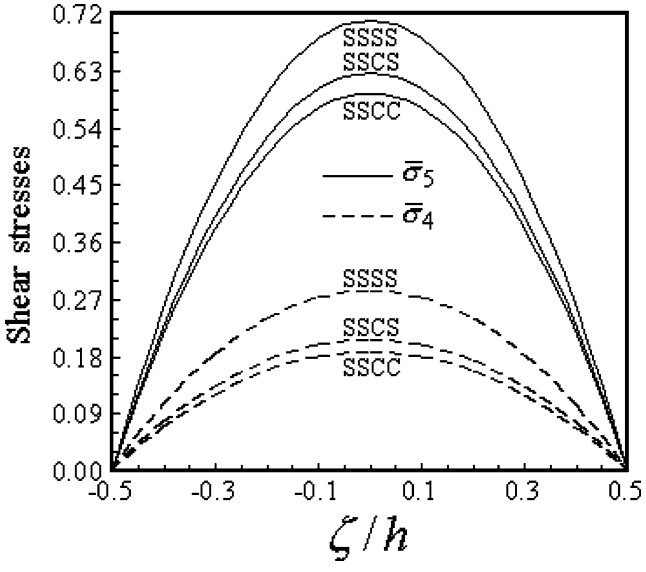

Fig. 8. Variation of the shear stresses $\bar{\sigma}_4$ and $\bar{\sigma}_5$ through the thickness of monoclinic spherical shells for various boundary conditions (*a/h*=10)

Table 8 shows the deflections and stresses obtained for a monoclinic square spherical shell under a uniformly distributed loading with a total of 45-term series using MFST and CST. The fundamental frequencies and uniaxial and biaxial critical buckling loads are also included in Table 8. Figs. 2–7 contain plots of non-dimensionalized center deflections $\bar{w}$, in-plane stresses $\bar{\sigma}_1$ and $\bar{\sigma}_2$, fundamental frequencies $\bar{\Omega}$, and uniaxial $\bar{\beta}_0$ and biaxial $\bar{\beta}_1$ critical buckling loads as functions of the thickness-to-side ratio for various boundary conditions. It should be pointed out that neglection of transverse shear strains in spherical shells could lead to an underprediction of the deflections (see Fig. 2) and an overprediction of the natural frequencies (see Fig. 5) and buckling loads (see Figs. 6 and 7). This is due to the low transverse shear modulus compared to the in-plane Young's moduli. Note that the differences between the CST and MFST results increase as the thickness of the shell is increased (i.e., the a/h parameter is decreased) irrespective of the considered boundary conditions. In Fig. 8 the through-thickness variations of the shear stresses $\bar{\sigma}_4$ and $\bar{\sigma}_5$ are presented. It is clear that other first-order shear deformation theories account for constant transverse shear stresses through the thickness and, therefore, require a correction to the transverse shear stiffness.

6 Conclusions

The mixed variational formulation is used to develop both analytical and numerical solutions for anisotropic elastic spherical shells according to the refined first-order shell theory. The shell is considered to be subjected to a uniformly distributed transverse load as well as to in-plane edge forces. Numerical results are presented for natural frequencies, critical buckling loads, deflections and stresses of spherical shells subjected to various edge conditions. The refined mixed first-order shear deformation shell theory (MFST) as well as the classical shell theory (CST) was used and results were compared. The results of MFST and CST are in close agreement with available solutions in the literature. The inclusion of transverse shear in the MFST overpredicts deflections and underpredicts frequencies and critical loads when compared with the results from CST especially for moderately thick shells. Moreover, the present MFST leads to the quadratic distribution of the transverse shear stresses (and zero transverse normal strain) and, therefore, no shear correction factors are used.

References

1. **Flügge, W.**: Stresses in shells. Berlin, Springer (1962)
2. **Ambartsumian, S.A.**: Theory of anisotropic shells. Washington, DC, NASA TTF-118 (1964)
3. **Kraus, H.**: Thin elastic shells. New York, Wiley (1967)
4. **Librescu, L.**: Elastostatics and kinetics of anisotropic and heterogeneous shell-type structures. The Netherlands, Noordhoff, Leyden (1975)
5. **Reddy, J.N.**: Exact solutions of moderately thick laminated shells. J Eng Mech 110 (1984) 794–809
6. **Reddy, J.N.; Liu C.F.**: A higher-order shear deformation theory of laminated elastic shells. Int J Eng Sci 23 (1985) 319–330
7. **Bhaskar, K.; Varadan, T.K.**: Exact elasticity solution for laminated anisotropic cylindrical shell. J Appl Mech 60 (1993) 41–47
8. **Stephens, W.B.; Fulton, R.E.:** Axisymmetric static and dynamic buckling of spherical caps due to centrally distributed pressure. AIAA J 7 (1969) 2120–2126
9. **Ball, R.E.; Burt, J.A.:** Dynamic buckling of shallow spherical shells. J Appl Mech 40 (1973) 411–416
10. **Reddy, J.N.; Khdeir, A.A.:** Dynamic response of cross-ply laminated shallow shells according to a refined shear deformation theory. J Acoust Soc Am 85 (1989) 2423–2431
11. **Hsu, Y.S.; Reddy, J.N.; Bert, C.W.:** Thermoelasticity of circular cylindrical shells laminated of bimodulus composite materials. J Therm Stress 4 (1981) 155–177
12. **Khdeir, A.A.; Reddy, J.N.; Frederick, D.:** A study of bending, vibration and buckling of cross-ply circular cylindrical shells with various shell theory. Int J Eng Sci 27 (1989) 1337–1351
13. **Fares, M.E.; Allam, M.N.M.; Zenkour, A.M.:** Hamilton's mixed variational formula for dynamical problems of anisotropic elastic bodies. SM Arch 14 (1989) 103–114
14. **Zenkour, A.M.:** Vibration of axisymmetric shear deformable cross-ply laminated cylindrical shells–a variational approach. Int J Eng Sci 36 (1998) 219–231
15. **Zenkour, A.M.:** Stress analysis of axisymmetric shear deformable cross-ply circular laminated cylindrical shells. J Eng Math 40 (2001) 315–332
16. **Zenkour, A.M.; Fares, M.E.:** Thermal bending analysis of composite laminated cylindrical shells using a refined first-order theory. J Therm Stress 23 (2000) 505–526
17. **Reissner, E.:** The effect of transverse shear deformation on the bending of elastic plates. J Appl Mech 12 (1945) 69–77
18. **Niordson, F.I.:** Shell theory. Amsterdam, North-Holland (1985)
19. **Fares, M.E.; Zenkour, A.M.:** Mixed variational formula for the thermal bending of laminated plates. J Therm Stress 22 (1999) 347–365

20. **Zenkour, A.M.:** Natural vibration analysis of symmetrical cross-ply laminated elastic plates using mixed variational formulation. Eur. J. Mech. A, Solids 19 (2000) 469–485
21. **Fares, M.E.; Zenkour, A.M.; El-Marghany, M.Kh.:** Nonlinear thermal effects on the bending response of cross-ply laminated plates using refined first-order theory. Compos Struct. 49 (2000) 257–267
22. **Zenkour, A.M.:** Buckling and free vibration of elastic plates using simple and mixed shear deformation theories. Acta Mech 146 (2001) 183–197
23. **Bogdadnovich, A.E.; Pastore, C.M.:** Mechanics of textile and laminated composites with applications to structural analysis. London, Chapman & Hall (1996)
24. **Vlasov, V.Z.:** General theory of shells and its applications in engineering. Washington, DC, NASA TTF-99 (1964)
25. **Yang, T.Y.:** High order rectangular shallow shell finite element. J Eng Mech Div, ASCE 99:57–81 (1973)
26. **Srinivas, S.; Rao, A.K.:** Bending, vibration and buckling of simply supported thick orthotropic rectangular plates and laminates: Int J Solids Struct (1970) 1463–1481
27. **Reddy, J.N.:** A refined nonlinear theory of plates with transverse shear deformation. Int J Solids Struct 20 (1984) 745–752
28. **Librescu, L.; Khdeir, A.A.; Reddy, J.N.:** Further results concerning the dynamic response of shear deformable elastic orthotropic plates. ZAMM 17 (1990) 23–33

Appendix

The elements of the symmetric matrix $[K]$ are expressed as:

$$
\begin{aligned}
K_{11} &= A_{11}\lambda_i^2 f_3 g_1 + 2A_{16}\lambda_i\lambda_j f_6 g_4 + A_{66}\lambda_j^2 f_2 g_2,\\
K_{12} &= A_{16}\lambda_i^2 f_6 g_4 + (A_{12} f_5 g_5 + A_{66} f_2 g_2)\lambda_i\lambda_j + A_{26}\lambda_j^2 f_4 g_6,\\
K_{13} &= \frac{1}{R}\left[(A_{11}+A_{12})\lambda_i f_5 g_1 + (A_{16}+A_{26})\lambda_j f_4 g_4\right], \quad K_{14} = K_{15} = 0,\\
K_{22} &= A_{66}\lambda_i^2 f_2 g_2 + 2A_{26}\lambda_i\lambda_j f_4 g_6 + A_{22}\lambda_j^2 f_1 g_3,\\
K_{23} &= \frac{1}{R}\left[(A_{16}+A_{26})\lambda_i f_4 g_4 + (A_{12}+A_{22})\lambda_j f_1 g_5\right], \quad K_{24} = K_{25} = 0,\\
K_{33} &= \frac{1}{R^2}(A_{11}+2A_{12}+A_{22}) f_1 g_1 + A_{55}\lambda_i^2 f_2 g_1 + 2A_{45}\lambda_i\lambda_j f_4 g_4 + A_{44}\lambda_j^2 f_1 g_2,\\
K_{34} &= A_{45}\lambda_i f_4 g_4 + A_{44}\lambda_j f_1 g_2, \quad K_{35} = A_{55}\lambda_i f_2 g_1 + A_{45}\lambda_j f_4 g_4,\\
K_{44} &= D_{66}\lambda_i^2 f_2 g_2 + 2D_{26}\lambda_i\lambda_j f_4 g_6 + D_{22}\lambda_j^2 f_1 g_3 + A_{44} f_1 g_1,\\
K_{45} &= D_{16}\lambda_i^2 f_6 g_4 + (D_{12} f_5 g_5 + D_{66} f_2 g_2)\lambda_i\lambda_j + D_{26}\lambda_j^2 f_4 g_6 + A_{45} f_4 g_4,\\
K_{55} &= D_{11}\lambda_i^2 f_3 g_1 + 2D_{16}\lambda_i\lambda_j f_6 g_4 + D_{66}\lambda_j^2 f_2 g_2 + A_{55} f_2 g_1,
\end{aligned}
$$

where

$$
\begin{aligned}
f_1 &= \int_0^a [F(\lambda_i x_1)]^2 dx_1, \quad f_2 = \int_0^a [F'(\lambda_i x_1)]^2 dx_1, \quad f_3 = \int_0^a [F''(\lambda_i x_1)]^2 dx_1,\\
g_1 &= \int_0^b [G(\lambda_j x_2)]^2 dx_2, \quad g_2 = \int_0^b [G'(\lambda_j x_2)]^2 dx_2, \quad g_3 = \int_0^b [G''(\lambda_j x_2)]^2 dx_2,\\
f_4 &= \int_0^a F(\lambda_i x_1) F'(\lambda_i x_1) dx_1, \quad g_4 = \int_0^b G(\lambda_j x_2) G'(\lambda_j x_2) dx_2,\\
f_5 &= \int_0^a F(\lambda_i x_1) F''(\lambda_i x_1) dx_1, \quad g_5 = \int_0^b G(\lambda_j x_2) G''(\lambda_j x_2) dx_2,\\
f_6 &= \int_0^a F'(\lambda_i x_1) F''(\lambda_i x_1) dx_1, \quad g_6 = \int_0^b G'(\lambda_j x_2) G''(\lambda_j x_2) dx_2.
\end{aligned}
$$

The elements of the symmetric matrix $[L]$ are expressed as:

$$
\begin{aligned}
&L_{11} = I_1 f_2 g_1, \quad L_{15} = I_2 f_2 g_1, \quad L_{22} = I_1 f_1 g_2, \quad L_{24} = I_2 f_1 g_2,\\
&L_{33} = I_0 f_1 g_1, \quad L_{44} = I_3 f_1 g_2, \quad L_{55} = I_3 f_2 g_1,\\
&L_{12} = L_{13} = L_{14} = L_{23} = L_{25} = L_{34} = L_{35} = L_{45} = 0.
\end{aligned}
$$

All elements of the matrix $[N]$ are equal to zero except $N_{33} = \lambda_i^2 f_2 g_1 + \gamma\lambda_j^2 f_1 g_2$.